LETTERS

Nanoscale double emulsions stabilized by single-component block copolypeptides

Jarrod A. Hanson[1], Connie B. Chang[2], Sara M. Graves[2], Zhibo Li[1], Thomas G. Mason[2,3,4] & Timothy J. Deming[1,2,4]

Water-in-oil-in-water emulsions are examples of double emulsions, in which dispersions of small water droplets within larger oil droplets are themselves dispersed in a continuous aqueous phase[1–3]. Emulsions occur in many forms of processing and are used extensively by the foods, cosmetics and coatings industries. Because of their compartmentalized internal structure, double emulsions can provide advantages over simple oil-in-water emulsions for encapsulation, such as the ability to carry both polar and non-polar cargos, and improved control over release of therapeutic molecules[4–6]. The preparation of double emulsions typically requires mixtures of surfactants for stability; the formation of double nanoemulsions, where both inner and outer droplets are under 100 nm, has not yet been achieved[7–9]. Here we show that water-in-oil-in-water double emulsions can be prepared in a simple process and stabilized over many months using single-component, synthetic amphiphilic diblock copolypeptide surfactants. These surfactants even stabilize droplets subjected to extreme flow, leading to direct, mass production of robust double nanoemulsions that are amenable to nanostructured encapsulation applications in foods, cosmetics and drug delivery.

Although they offer certain advantages over ordinary oil-in-water emulsions, stable water-in-oil-in-water (WOW) emulsions generally do not form spontaneously with a single surfactant and standard emulsification methods[7,10]. Microfluidics can be used to make double emulsions that are micrometres in size and highly uniform[8,9], yet the throughput can be low compared with commercial processes for making polydisperse single emulsions[11]. Typical methods for making WOW emulsions use a two-step process of first forming an 'inverse' water-in-oil emulsion, followed by emulsification of this mixture in water using a combination of surfactants[2,3,7,12,13]. This process allows control of both droplet volumes if the emulsions are made monodisperse[3], yet cannot form stable nanoscale droplets and requires a difficult search for surfactant combinations that can coexist without destabilizing either inner or outer droplet interfaces[2]. Consequently, improving stability and reducing droplet sizes are the key challenges in the development of double emulsions for applications[14].

The block copolypeptide surfactants we designed have the general structure poly(L-lysine·HBr)$_x$-*b*-poly(*racemic*-leucine)$_y$, K$_x$(*rac*-L)$_y$, where x ranged from 20 to 100, and y ranged from 5 to 30 residues (Fig. 1a, Supplementary Information). The hydrophilic poly(L-lysine·HBr) segments are highly charged at neutral pH, provide good water solubility[15] and possess abundant amine groups for chemical functionalization[16]. Unlike hydrophobic segments of other polymeric amphiphiles, poly(L-leucine) segments adopt rod-like α-helical conformations that give rise to strong interchain associations and poor solubility in common organic solvents[17]. Block copolymers of the structure K$_x$L$_y$ (for example K$_{60}$L$_{20}$, Fig. 1b) associate strongly in water to form membranes through packing of the hydrophobic segments[18]. Consequently, we focused on poly(*rac*-leucine) because its disordered chain conformation improves solubility (Supplementary Table 1)[19,20] and helps to promote surface activity (Supplementary Table 1), and its peptidic nature allows for additional mechanical stabilization of droplet interfaces through interchain hydrogen-bonding in the oil phase[21].

We screened diblock copolypeptides for emulsification activity by adding silicone oil to aqueous K$_x$(*rac*-L)$_y$ solutions (Supplementary Table 1, Supplementary Figs 2a–c, 5a). The resulting mixtures were sheared using a hand-held rotary homogenizer and then passed six times through a high-pressure microfluidic homogenizer (Fig. 1c). All K$_x$(*rac*-L)$_y$ samples gave stable WOW nanoemulsions that did not ripen (that is, coarsen in size) or phase-separate for over nine months. Only copolypeptides with low hydrophobic content, for example K$_{40}$(*rac*-L)$_5$, gave emulsions that slowly phase-separated after one year. Other methods of mixing, including ultrasonic

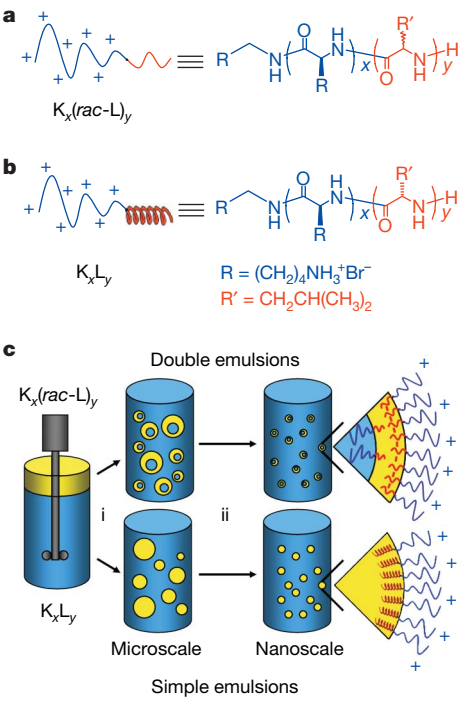

Figure 1 | Structures of block copolypeptide surfactants and emulsification procedure. a, K$_x$(*rac*-L)$_y$. **b**, K$_x$L$_y$. **c**, Emulsification procedure used to generate both simple and double emulsions. Step (i), ultrasonic or hand-held homogenization; step (ii), microfluidic homogenization. Yellow represents the oil phase, blue the aqueous phase containing block copolypeptide surfactant.

[1]Bioengineering Department, [2]Department of Chemistry and Biochemistry, [3]Department of Physics and Astronomy, and [4]California NanoSystems Institute, University of California, Los Angeles, California 90095, USA.

mixing, also provided stable emulsions, but with droplets up to several micrometres in diameter (Fig. 1c). Use of hydrophobic segments longer than 30 residues greatly diminished aqueous solubility (Supplementary Table 1); for instance, $K_{40}(rac\text{-}L)_{30}$ could only be dissolved up to 1 mM. As controls, we also used 0.1 mM suspensions of $K_{60}L_{20}$ and K_{60} as surfactants: $K_{60}L_{20}$ did form stable emulsions and K_{60} failed to emulsify oil and water mixtures (Supplementary Fig. 4). These results indicated that $K_x(rac\text{-}L)_y$ surfactants give stable emulsions over a broad range of compositions and concentrations.

To probe droplet structure, we imaged block-copolypeptide-stabilized emulsions by using optical microscopy and cryogenic transmission electron microscopy (CTEM). All samples with $K_x(rac\text{-}L)_y$ were found to contain oil droplets, each containing predominately a single internal aqueous droplet with consistent inner to outer volume ratios (Fig. 2a, Supplementary Figs 2, 3). In contrast, the emulsions formed using $K_{60}L_{20}$ contained only simple oil droplets (Fig. 2b), revealing that the racemic-leucine segments play a key part in stabilizing the double emulsion structure. As copolypeptide hydrophobic content was decreased, droplet sizes increased (Supplementary Table 1, Supplementary Fig. 5c), suggesting that copolymer composition influences interfacial mean curvature. Average droplet diameters also increased when the concentration of $K_{40}(rac\text{-}L)_{20}$ was decreased (Supplementary Fig. 5a). Likewise, decreasing the volume fraction of oil yielded smaller emulsion droplets (Supplementary Fig. 5b). Emulsions always formed such that water remained the continuous phase and did not invert up to oil volume fractions approaching 50%. In addition to polydimethylsiloxane (PDMS), other immiscible liquids such as dodecane, soybean oil and methyl oleate gave emulsions using 1 mM $K_{40}(rac\text{-}L)_{20}$ in water. The versatility of our design was shown by formation of stable emulsions using $R_{40}(rac\text{-}L)_{10}$ or $E_{40}(rac\text{-}L)_{10}$, containing guanidinium or carboxylate functionality of L-arginine (R) and L-glutamate (E), respectively (Supplementary Fig. 3a, b).

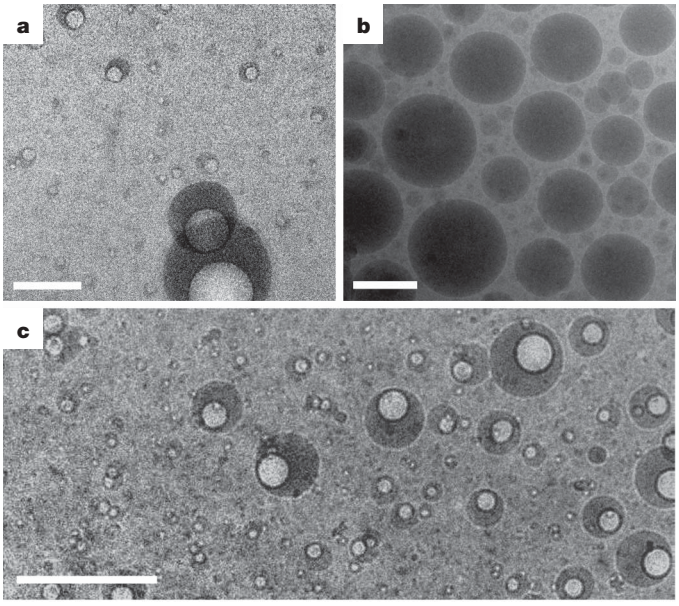

Figure 2 | Cryogenic transmission electron microscopy of copolypeptide-stabilized emulsions prepared using a microfluidic homogenizer. Vitrified water gives a light background and silicone oil appears dark and provides contrast. Emulsions prepared under the following conditions: number of passes $N = 6$, homogenizer inlet air pressure $P = 130$ p.s.i., block copolypeptide concentration $C = 1.0$ mM, and oil volume fraction $\phi = 0.20$. **a**, Image of a WOW double emulsion stabilized by $K_{40}(rac\text{-}L)_{20}$. **b**, Image of a single oil-in-water emulsion stabilized by $K_{60}L_{20}$. **c**, Image of size-fractionated droplets isolated from a $K_{40}(rac\text{-}L)_{20}$-stabilized double emulsion by low-speed centrifugation followed by ultracentrifugation. All scale bars, 200 nm.

Formation of nanoscale emulsion droplets is necessary for many applications, such as drug delivery where the outer droplet diameter generally needs to be less than 200 nm, and preferably between 50 nm and 100 nm (ref. 22). Although many methods are available for preparation of double emulsions, none allows preparation of outer droplets in this size range[7–9,14]. We used ultrasonic homogenization to prepare a $K_{40}(rac\text{-}L)_{20}$ emulsion yielding a polydisperse sample with the smallest double emulsion droplets observed by CTEM being around 400 nm in diameter. These droplets were further reduced in size by passage six times through a microfluidic homogenizer, yielding droplet diameters ranging from about ten to a few hundred nanometres. The stability of these double emulsions against both external and internal coalescence allowed the use of centrifugation to fractionate droplets into a desired size range. Centrifugation of the sample in Fig. 2a gave a buoyant fraction containing droplets hundreds of nanometres in diameter. The smaller droplets in the remaining suspension were further separated by ultracentrifugation[11], yielding a fraction with droplets ranging from about 10 to 100 nm in diameter (Fig. 2c). This fractionation procedure shows that isolation of stable double emulsion droplets in the nanoscale range is feasible, and that they are remarkably stable to shear.

To demonstrate their encapsulating ability, we loaded both water-soluble and oil-soluble fluorescent markers into copolypeptide-stabilized double emulsions. Water-soluble InGaP/ZnS quantum dots were mixed with fluorescein-labelled $K_{40}(rac\text{-}L)_{10}$ before emulsification with silicone oil containing pyrene. Using fluorescence microscopy, we imaged both markers and the labelled polypeptide in the double emulsion droplets (Fig. 3a). The images also showed the compartmentalization of hydrophilic quantum dots (red) into the inner aqueous phase, hydrophobic pyrene (blue) into the oil phase and the labelled polypeptide (green) stabilizing the outer interface. Polypeptide at the inner interface was not observed, probably owing to quenching of the fluorescein label by the quantum dots. In samples prepared with $K_{60}L_{20}$ surfactant, we observed only simple oil droplets with no internal aqueous compartment (Fig. 3b). These cargos remained encapsulated within the droplets for at least three months, showing unprecedented stability of the inner aqueous compartment compared with other double emulsion systems[4,7,14].

Our $K_x(rac\text{-}L)_y$ surfactants were designed with high hydrophilic contents, namely the ratio of hydrophilic to hydrophobic residues, which favour stabilization of oil-in-water emulsions where the oil is

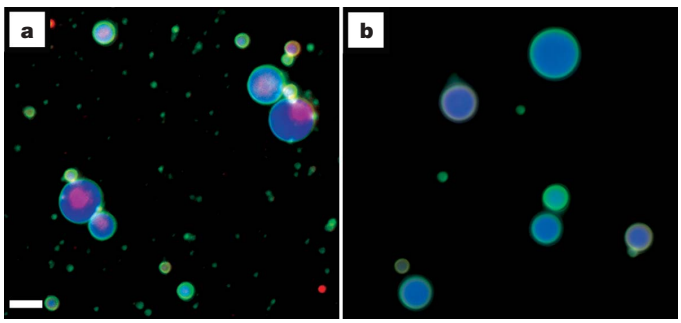

Figure 3 | Fluorescence micrographs of double emulsions containing polar and non-polar cargos. Samples were prepared using an ultrasonic homogenizer (10 s at 35% power) with $\phi = 0.2$ and $C = 0.1$ mM. The oil phase fluoresces blue because of entrapped pyrene (0.01 M), and the internal aqueous phase fluoresces red because of encapsulation of InGaP quantum dots (2 μM). The polypeptides are labelled with fluorescein isothiocyanate (FITC) and therefore fluoresce green. Before imaging, the droplets were dialysed against and subsequently diluted with pure water to remove red fluorescence from the external phase (see Supplementary Information). **a**, Double emulsion stabilized by FITC-labelled $K_{40}(rac\text{-}L)_{10}$, loaded with both pyrene and quantum dots. **b**, Single emulsion stabilized by FITC-labelled $K_{60}L_{20}$, loaded with both pyrene and quantum dots. Scale bars, 5 μm.

on the concave side of the curved interface of a nanoscale droplet. Conversely, the inner water–oil interface of a WOW double emulsion is best stabilized by a surfactant with a low hydrophilic content because the oil is on the convex side of the interface. The opposite signs of these mean interfacial curvatures[23] explain why single-component surfactants generally do not stabilize double emulsion droplets and combinations of surfactants are required[2]. This also explains the formation of only oil-in-water emulsions with $K_{60}L_{20}$, because the rod-like oligoleucine segments are poorly solvated by the oil and aggregate in the oil phase[17]. To stabilize an inner aqueous droplet in a WOW double emulsion, the hydrophobic polypeptide segments need to disperse in the oil to prevent steric crowding of the large hydrophilic segments in the aqueous phase (Fig. 1c).

The racemic-leucine segments in $K_x(rac\text{-L})_y$ provide a combination of features that stabilize double emulsion droplets. The conformational flexibility of these segments improves oil solubility, because poly(*rac*-leucine) is soluble in organic solvents such as CH_2Cl_2 and $(CH_3)_2SO$ whereas poly(L-leucine) is not[19,20]. This allows $K_x(rac\text{-L})_y$ chains to stabilize the oil–water interface better in the inner droplet as the hydrophobic segments can disperse more readily in the oil. Despite its improved solubility, in an oil solvent nearly all residues of poly(*rac*-leucine) will also be engaged in both intramolecular and intermolecular hydrogen bonds. Studies on racemic polymers of both leucine and phenylalanine have demonstrated that they associate in organic solvents through hydrogen bonding[21]. At the interface of an inner aqueous droplet with oil, the high hydrophilic content of our polymers favours a low packing density of *rac*-leucine segments in the oil phase that would allow few interchain hydrogen bonds and give a weakly stabilized interface (Fig. 1c). But the opposite curvature of the oil–water interface in the outer droplet allows dense packing of the *rac*-leucine segments in the oil phase, favouring interchain hydrogen bonding. Consequently, even though inner aqueous droplets are likely to be unstable, they are prevented from merging with the outer droplets, and forming simple emulsions, as the outer interfaces are expected to be reinforced by hydrogen-bond cross-linking. To test this concept, emulsions were prepared containing a silicone oil capped with acetamide groups capable of hydrogen bonding to *rac*-leucine segments. Emulsification with $K_{60}(rac\text{-L})_{20}$ gave WOW nanoemulsions containing multiple internal droplets (Supplementary Fig. 6), supporting the hypothesis that *rac*-leucine segments can stabilize droplets through hydrogen bonding interactions in the oil phase, thus inhibiting internal droplet coalescence.

Our use of racemic, disordered hydrophobic polypeptide segments that interact through hydrogen bonding is a new means of stabilizing WOW double emulsions. This approach differs greatly from protein- and peptide-stabilized emulsions where double emulsions do not form without the use of additional surfactants, and an ordered amphiphilic helix is the most common source of surface activity[24–28]. Our strategy also can be applied to other copolypeptides, because samples containing *rac*-valine and *rac*-alanine hydrophobic segments also gave stable double nanoemulsions (Supplementary Fig. 3b,c). Use of block copolypeptide surfactants overcomes key limitations of WOW double emulsions by allowing the straightforward preparation of stable nanoscale droplets that can simultaneously encapsulate both oil-soluble and water-soluble cargos.

METHODS SUMMARY

We first dissolved $K_{40}(rac\text{-L})_{20}$ copolypeptide in ultrapure water at the desired concentration (0.01–1.5 mM). Silicone oil (viscosity 0.1 $cm^2\,s^{-1}$) was added to give the desired volume fraction (ϕ) of oil in the continuous phase ($0.05 < \phi < 0.50$). We prepared a microscale emulsion either by mixing for 1 min using a hand-held homogenizer (IKA Ultra-Turrax T8 with the S8N-8G dispersing element) or by mixing for 10 s using a hand-held ultrasonic homogenizer (Cole-Parmer 4710 Series Model ASI at an output of 35–40%). This emulsion was then passed through a processor (M-110S Microfluidizer) with a 75-μm stainless steel/ceramic interaction chamber and an input air pressure (P) of 130 p.s.i. The emulsion was collected at the product outlet, and then passed through the microfluidic homogenizer repeatedly for a total of six passes ($N = 6$), which decreased the average droplet radius $\langle a \rangle$ and increased the monodispersity of the sample. We used a similar protocol for emulsions generated using other block copolypeptide surfactants (Supplementary Table 1, Supplementary Fig. 2a–c). The ratio of inner droplet radius to outer droplet radius was relatively uniform for different hydrophobic chain lengths at about 0.5 (Supplementary Table 1, Supplementary Fig. 2d). Other amphiphilic block copolypeptides where either the lysine or leucine domains were substituted with different hydrophilic or hydrophobic residues, respectively, also formed double emulsions (Supplementary Fig. 3a–d). We also qualitatively evaluated the emulsification capability of different polypeptide surfactants using toluene, which forms less stable emulsions, and with a control homopolypeptide, K_{60} (Supplementary Fig. 4).

Full Methods and any associated references are available in the online version of the paper at www.nature.com/nature.

Received 13 December 2007; accepted 23 June 2008.

1. Bibette, J., Calderon, F. L. & Poulin, P. Emulsions: Basic principles. *Rep. Prog. Phys.* **62,** 969–1033 (1999).
2. Ficheux, M. F., Bonakdar, L., Leal-Calderon, F. & Bibette, J. Some stability criteria for double emulsions. *Langmuir* **14,** 2702–2706 (1998).
3. Wang, Y. F., Tao, Z. & Gang, H. Structural evolution of polymer-stabilized double emulsions. *Langmuir* **22,** 67–73 (2006).
4. Pays, K. *et al.* Double emulsions: how does release occur? *J. Control. Release* **79,** 193–205 (2002).
5. Davis, S. S. & Walker, I. M. Multiple emulsions as targetable delivery systems. *Methods Enzymol.* **149,** 51–64 (1987).
6. Okochi, H. & Nakano, M. Preparation and evaluation of W/O/W type emulsions containing vancomycin. *Adv. Drug Deliv. Rev.* **45,** 5–26 (2000).
7. Garti, N. Double emulsions: Scope, limitations and new achievements. *Colloids Surf. A* **123,** 233–246 (1997).
8. Loscertales, I. G. *et al.* Micro/nano encapsutation via electrified coaxial liquid jets. *Science* **295,** 1695–1698 (2002).
9. Utada, A. S. *et al.* Monodisperse double emulsions generated from a microcapillary device. *Science* **308,** 537–541 (2005).
10. Morais, J. M., Santos, O. D. H., Nunes, J. R. L., Zanatta, C. F. & Rocha-Filho, P. A. W/O/W multiple emulsions obtained by one-step emulsification method and evaluation of the involved variables. *J. Disp. Sci. Technol.* **29,** 63–69 (2008).
11. Mason, T. G., Wilking, J. N., Meleson, K., Chang, C. B. & Graves, S. M. Nanoemulsions: formation, structure, and physical properties. *J. Phys. Condens. Matter* **18,** R635–R666 (2006).
12. Goubault, C. *et al.* Shear rupturing of complex fluids: Application to the preparation of quasi-monodisperse water-in-oil-in-water double emulsions. *Langmuir* **17,** 5184–5188 (2001).
13. Okushima, S., Nisisako, T., Torii, T. & Higuchi, T. Controlled production of monodisperse double emulsions by two-step droplet breakup in microfluidic devices. *Langmuir* **20,** 9905–9908 (2004).
14. Benichou, A., Aserin, A. & Garti, N. Double emulsions stabilized with hybrids of natural polymers for entrapment and slow release of active matters. *Adv. Colloid Interface Sci.* **108–109,** 29–41 (2004).
15. Katchalski, E. & Sela, M. Synthesis and chemical properties of poly-alpha-amino acids. *Adv. Protein Chem.* **13,** 243–492 (1958).
16. Niederhafner, P., Šebestík, J. & Ježek, J. Peptide dendrimers. *J. Pept. Sci.* **11,** 757–788 (2005).
17. Nowak, A. P. *et al.* Rapidly recovering hydrogel scaffolds from self-assembling diblock copolypeptide amphiphiles. *Nature* **417,** 424–428 (2002).
18. Holowka, E. P., Pochan, D. J. & Deming, T. J. Charged polypeptide vesicles with controllable diameter. *J. Am. Chem. Soc.* **127,** 12423–12428 (2005).
19. Kricheldorf, H. R. & Mang, T. C-13-NMR sequence-analysis, 20. Stereospecificity of the polymerization of D,L–Leu-NCA and D,L–Val-NCA. *Makromol. Chem.: Macromol. Chem. Phys.* **182,** 3077–3098 (1981).
20. Breitenbach, J. W., Allinger, K. & Koref, A. Viskositätsstudien an Lösungen von DL-Phenylalanin-Polypeptiden. *Monatsh. Chem.* **86,** 269 (1955).
21. Lapp, C. & Marchal, J. Preparation de la poly-D,L-phenylalanine en helice par polymerisation de la D,L-benzyl-4 oxazolidine dione-2–5. *J. Chim. Phys.* **60,** 756–766 (1963).
22. Kataoka, K., Kwon, G. S., Yokoyama, M., Okano, T. & Sakurai, Y. Block-copolymer micelles as vehicles for drug delivery. *J. Control. Release* **24,** 119–132 (1993).
23. Strey, R. Microemulsion microstructure and interfacial curvature. *Colloid Polym. Sci.* **272,** 1005–1019 (1994).
24. Enser, M., Bloomberg, G. B., Brock, C. & Clark, D. C. De novo design and structure−activity relationships of peptide emulsifiers and foaming agents. *Int. J. Biol. Macromol.* **12,** 118–124 (1990).
25. Dickinson, E. Structure and composition of adsorbed protein layers and the relationship to emulsion stability. *J. Chem. Soc., Faraday Trans.* **88,** 2973–2983 (1992).
26. Saito, M., Ogasawara, M., Chikuni, K. & Shimizu, M. Synthesis of a peptide emulsifier with an amphiphilic structure. *Biosci. Biotechnol. Biochem.* **59,** 388–392 (1995).

27. Dalgleish, D. G. Conformations and structures of milk proteins adsorbed to oil–water interfaces. *Food Res. Intl* **29,** 541–547 (1996).
28. Chang, C. B., Knobler, C. M., Gelbart, W. M. & Mason, T. G. Curvature dependence of viral protein structures on encapsidated nanoemulsion droplets. *ACS Nano* **2,** 281–286 (2008).

Supplementary Information is linked to the online version of the paper at www.nature.com/nature.

Acknowledgements This work is supported by a grant from the National Science Foundation (T.J.D.), a grant from the Human Frontiers of Science Program (T.J.D.), and University of California start-up funds (T.J.D. and T.G.M.). Some of the work was conducted at the National Resource for Automated Molecular Microscopy (NRAMM) which is supported by the National Institutes of Health through the National Center for Research Resources P41 programme. We thank C. Potter and J. Quispe of NRAMM at the Scripps Research Institute, and S. Zhong and D. Pochan of the University of Delaware, for use of cryoelectron microscopy equipment.

Author Contributions J.A.H. synthesized the polypeptides, prepared and characterized the emulsions, designed experiments, and assisted in manuscript preparation. C.B.C and S.M.G. also prepared and characterized the emulsions. Z.L. imaged the emulsions using CTEM. T.G.M. and T.J.D. initiated the project, designed and supervised the experiments, analysed the data, and drafted the manuscript. T.J.D. assembled and finalized the manuscript. All authors discussed the results and commented on the manuscript.

Author Information Reprints and permissions information is available at www.nature.com/reprints. The authors declare competing financial interests: details accompany the full-text HTML version of paper on www.nature.com/nature. Correspondence and requests for materials should be addressed to T.J.D. (demingt@seas.ucla.edu) or T.G.M. (mason@chem.ucla.edu).

METHODS

Fractionation of emulsions. A $K_{40}(rac\text{-}L)_{20}$ emulsion, with block copolypeptide concentration $C = 1.5$ mM (prepared as in Methods Summary), was centrifuged in a 15 mL plastic centrifuge tube for 24 h at 3,500 r.p.m. using a tabletop centrifuge (IEC HN-S). A 0.5-mm plug was formed and separated from the remnant suspension beneath. The plug formed at the top of the tube because the density of silicone oil is lower than water (0.973 g ml^{-1} for 0.1 cm^2 s^{-1} silicone oil, 1.0 g ml^{-1} for water). The remnant suspension was further fractionated at 20,000 r.p.m. for 4 h using an ultracentrifuge (Beckman L8-55) with a swinging bucket rotor. The plug that formed on top of the suspension was separated and the remaining suspension was imaged using CTEM (Fig. 2c).

Dynamic light scattering. Because the interfacial organization of double emulsions is complex, describing their structure in complete detail can be complicated. Two different droplet size distributions are necessary for inner and outer droplets, $p_i(a_i)$ and $p_o(a_o)$, respectively, where a is the radius. Although the droplet volume fraction of the outer droplets is simply ϕ_o, the distribution of inner droplet volume fractions depends on $p_i(a_i)$ and on the number distribution of smaller droplets within a given droplet, $p_i(N_i)$, where N_i is the number of inner droplets. To simplify the description of double emulsions, usually average radii (for example, $\bar{a}_i$ and $\bar{a}_o$), inner volume fractions $\bar{\phi}_i$ and numbers of inner droplets $\bar{N}_i$ are reported, as quantifying the full distributions can be difficult. The outer diameters of emulsion droplets were estimated by dynamic light scattering (DLS) with a Photocor-FC board and software. Although DLS of double emulsions yields intensity correlation decay data that are complex[3], we believe the DLS data provide a crude estimate of average outer droplet diameter consistent with CTEM real-space data. Average outer droplet diameters from CTEM measurements were generally lower than diameters from DLS, reflecting the inevitable exclusion of larger droplets from the thin vitrified water layer (<200 nm) usable for CTEM imaging. The DLS samples were diluted to obtain an intensity reading of between 1×10^5 and 6×10^5 counts. Each sample was run at 90° scattering angle for 500 s, with linear channel spacing and an adjustable baseline. The fitting procedure used was cumulant analysis with an adjustable baseline to fit the data and calculate droplet radii. DLS data for different emulsion formulations are given in Supplementary Fig. 5.

Fluorescence microscopy. Before fluorescence imaging, emulsion suspensions were diluted tenfold with deionized water. A drop of emulsion was then placed on a glass slide and covered using a glass cover slip. The samples were imaged using a Zeiss Axiovert 200 fluorescence microscope equipped with ultraviolet filter set #49 (excitation 365 nm, emission 420 to 470 nm), blue filter set #10 (excitation 450 to 490 nm, emission 515 to 565 nm), and green filter set #43 (excitation 530 to 560 nm, emission 570 to 640 nm).

CTEM imaging. Each emulsion sample was diluted tenfold with deionized water before imaging. An aliquot of each sample (5 μl) was then placed on a Formvar stabilized with carbon 300 mesh copper grid (Ted Pella). The grid was loaded into a Vitrobot (FEI) automated vitrification device for automated sample blotting and vitrification in liquid ethane. The grid was stored under liquid nitrogen and then placed, using a cold stage, in a Phillips Tecnai F20 electron microscope and imaged with an accelerating voltage of 120 kV. Images were obtained on a Teitz SCX slow-scan CCD detector controlled by the Leginon software package[29].

Critical aggregation concentration via pyrene fluorescence. Polypeptide solutions (2 ml) were dispersed in water at a range of concentrations (2.0×10^{-3} to 2.0×10^{-12} M). A stock pyrene solution was made by dissolving pyrene in acetone (6.0×10^{-2} M). Next, an appropriate amount of the pyrene stock solution was added to give a final concentration of 12×10^{-7} M in water and the acetone was evaporated off. To each polypeptide solution, we added 2.0 ml of the stock pyrene solution to afford a final concentration of 6.0×10^{-7} M. Each solution was allowed to equilibrate overnight before measurements. To record fluorescence spectra, we added 3.0 ml of each polypeptide solution to a polystyrene cuvet (4.0 ml). The excitation spectra were recorded within a range of 300–360 nm at an emission wavelength of 390 nm. All spectra were run with an integration time of 1 s per 0.5 nm. The ratio of the intensities of two peaks I_{338}/I_{333} was plotted as a function of polypeptide concentration (M) for each sample. The critical aggregation concentrations were determined as the intersection of the extrapolated straight line fits of the plot as previously described[18].

Interfacial tension measurements. Interfacial tension (γ) values between polypeptide solutions (0.1 mM $K_{60}L_{20}$ and 0.1 mM $K_{40}(rac\text{-}L)_{20}$) and PDMS (0.1 cm^2 s^{-1}) were measured using the Du Nouy ring method outlined by Zuidema and Waters[30]. A platinum–iridium ring (circumference 5.0 cm) was attached to a balance and the mass of the oil/polypeptide solution interface was measured as the ring was pulled at a rate of 0.01 mm s^{-1} using a calibrated bottom-hole balance apparatus at 25 °C. The polypeptide solutions ($K_{60}L_{20}$ and $K_{40}(rac\text{-}L)_{20}$) were well above their measured critical aggregation concentration values of 7.1×10^{-7} and 9.7×10^{-7} M, respectively. To reduce wall effects, the diameter of the container (8.0 cm) was significantly larger than the diameter of the Du Nouy ring. In addition, each polypeptide solution was equilibrated with the oil–water interface for at least 24 h before measurement.

29. Carragher, B. *et al.* Leginon: An automated system for acquisition of images from vitreous ice specimens. *J. Struct. Biol.* **132**, 33–45 (2000).
30. Zuidema, H. H. & Waters, G. W. Ring method for the determination of interfacial tension. *Ind. Eng. Chem. Anal. Edn* **13**, 312–313 (1941).